Astron. Astrophys. 219, 271–275 (1989)

ASTRONOMY AND ASTROPHYSICS

Eclipse cross-sections of cool components in double star systems

H. Isliker, H. Nussbaumer, and M. Vogel

Institute of Astronomy, ETH Zentrum, CH-8092 Zürich, Switzerland

Received November 23, 1988; accepted February 14, 1989

Summary. We give explicit expressions for Raman and Rayleigh scattering cross-sections. For the case of Rayleigh scattering we derive an analytical expression describing the attenuation of continuum and line radiation by a cool stellar wind. The process is of particular importance in double star systems, where observed eclipses can yield information on the geometrical configuration of the system. Observed variations in line ratios might mimic changes in the degree of ionization during a revolution period, whereas they could well be due to the strong wavelength dependence of Rayleigh scattering. The eclipse effects are also a means of estimating mass-loss, as shown with the example of the symbiotic star BF Cyg.

We also investigate the fluorescence mechanism in which Fe^+ absorbs the $\lambda 1548$ component in the C IV $\lambda 1550$ doublet.

Key words: binaries – symbiotic stars – Rayleigh scattering – C IV, Fe II

1. Introduction

Eclipse effects in double star systems can help in deriving spatial properties of the configuration. This possibility is particularly viable when the object appears as a pointlike source. We shall calculate the cross-section which a cool giant presents in the far UV above Ly α up to 2000 Å. In that range radiation is mainly affected by Rayleigh-scattering. In addition to continuum scattering – which for eclipsing systems is as effective as true absorption – we also investigate the influence of the Fe II line absorption in the transition $a\,^4F_{9/2} - y\,^4H^0_{11/2}$ at 1548.2 Å. It has been suggested that this absorption might be responsible for the weakening of the $2s\,^2S_{1/2} - 2p\,^2P^0_{3/2}$ component in the C IV resonance doublet (Johansson, 1983).

The present study was initiated in view of investigating symbiotic stars. However, the results are valid for any double star system, where one of the components is a mass-losing red giant, and where Rayleigh scattering is the dominant attenuation process for the 1216 Å to 2000 Å continuum.

2. The astronomical model

We intend to solve the following problem: What is the "size" of a mass-losing red giant in a double star system, when seen at wavelengths between Ly α and 2000 Å. M-giants or Mira-type variables possess extended shells which are possible sources of opacity for lines and continuum; it is generally accepted that they are the cool component in symbiotic systems.

We define s as the radial distance to a line of sight from the center of the star. In this work we shall calculate the distances – they depend on λ – for which the optical depth along the line of sight reaches the value $\tau_\lambda(s) = 1$. We are primarily concerned with double star configurations where the red giant may be losing mass at a high rate $\dot{M}$, and we therefore calculate $\tau_\lambda(s)$ as a function of $\dot{M}$. Thus we have to know the absorption and scattering properties of the outer atmosphere and wind of a mass-losing red giant.

We divide the extended atmosphere of the giant into two parts: the photosphere and the wind. In the wind the radial dependence of the electron temperature, T_e, and the hydrogen density, N, are calculated on the assumption of spherical symmetry, constant mass-loss and a velocity law $v(r)$, with the asymptotic behaviour

$$v(r) = v_\infty \quad \text{for } r \to \infty\,, \tag{1}$$

where r denotes the radial distance from the center of the mass-losing star. The abundances are assumed to be cosmic. The optical depth, τ, in the continuum along the line of sight at distance s is

$$\tau(s) = \int_{-\infty}^{\infty} \sigma N(t)\, dt\,, \tag{2}$$

where σ is the absorption cross-section, and t is the geometrical coordinate along the line of sight, with $t = 0$ as the point nearest to the star. We need in particular the radial dependence of N and T_e. In a steady state the hydrogen density in the wind is a function of $\dot{M}, v(r)$ and r. In the region where $v(r) = v_\infty$ the density decreases $\sim 1/r^2$:

$$N(r) = \frac{\dot{M}}{4\pi\,\mu m_H v(r)}\,\frac{1}{r^2} = N(\tilde{R})\left(\frac{\tilde{R}}{r}\right)^2, \tag{3}$$

μm_H is the mean molecular weight of the gas. The temperature is assumed to be given by

$$T_e(r) = T_e(\tilde{R})\left(\frac{\tilde{R}}{r}\right)^{1/2}. \tag{4}$$

The transition point $\tilde{R}$ is defined as the point where the density of the Scholz model falls below the wind density. For $r \leqq \tilde{R}$ we read $N(r)$ and $T_e(r)$ from the extended static model atmosphere for M-giants, provided by Scholz; they are described in Scholz (1985), details about the opacity sources are given in Scholz and Tsuji (1984).

Send offprint requests to: H. Nussbaumer

3. Opacities

3.1. Opacity sources in the continuum

We restrict optical depth calculations to wavelengths observable with the shortwavelength spectrograph on IUE. We therefore neglect molecular band absorbers which become important at longer wavelengths, and whose opacities are only known in the atmosphere but not in the wind. In order to study their relative importance we take in a preliminary numerical calculation the following absorption and scattering mechanisms into account: hydrogen free-free and bound-free absorption, Thomson scattering by free electrons, bound-free and free-free absorption by H^-, photoionization by some metals, Rayleigh and Raman scattering by hydrogen.

For Rayleigh scattering different and conflicting scattering coefficients are given and employed in the literature, and for Raman scattering we have not found a readily applicable formula for astrophysical applications. We have therefore derived the necessary expressions from first principles. Rayleigh scattering may be regarded as a two-photon process. It is a special case of Raman scattering for which the differential cross-section $d\sigma$ for scattering of photons into the solid angle $d\Omega$ is

$$\frac{d\sigma}{d\Omega} = \left(\frac{2\pi e}{c}\right)^4 \nu_i \nu_f^3 \left|\sum_m \left[\frac{(\boldsymbol{D}_{fm}\cdot\boldsymbol{\lambda}_f^*)\,(\boldsymbol{D}_{mi}\cdot\boldsymbol{\lambda}_i)}{\varepsilon_i-\varepsilon_m+h\nu_i} + \frac{(\boldsymbol{D}_{fm}\cdot\boldsymbol{\lambda}_i)\,(\boldsymbol{D}_{mi}\cdot\boldsymbol{\lambda}_f^*)}{\varepsilon_i-\varepsilon_m-h\nu_f}\right]\right|^2. \quad (5)$$

This formula is derived by a second order time-dependent perturbation theory. Initial, intermediate and final states are expanded in terms of stationary states which are solutions of the time-independent Schrödinger equation. This implies infinite lifetimes for the states involved. As a consequence of this assumption differential cross-sections have singularities at $|\varepsilon_i-\varepsilon_m| = h\nu$. A more rigorous treatment includes a term for radiation damping which avoids these singularities at resonance energies. The neglect of radiative damping is well justified in our case, as we are interested in the general continuum and not in particular effects close to lines. The complete expansion (5) includes bound state as well as continuum state functions. The formula describes the general process of scattering. An incident photon of a given energy $h\nu_i$ and polarisation vector $\boldsymbol{\lambda}_i$ is absorbed by the atom in the initial state $|i\rangle$ with eigenenergy ε_i. The absorption leads to an intermediate state $|q\rangle$. In Raman scattering another photon of different energy $h\nu_f$ and polarisation vector $\boldsymbol{\lambda}_f$ is emitted, leaving the atom in a state $|f\rangle$ with ε_f. In Rayleigh scattering initial and final atomic states have the same energy. The dipole matrix element $\boldsymbol{D}_{lk}$ represents the action of the dipole operator $e\boldsymbol{R}$:

$$e\boldsymbol{D}_{lk} = \langle k|e\boldsymbol{R}|l\rangle\,. \quad (6)$$

We give now the explicit formula for Raman scattering in the case where the initial state is $1s^2S$. As the dipole operator acts twice, initial and final states have the same parity. The ground term of hydrogen is of even parity, the intermediate states are of odd parity, angular momentum can be changed by 1 in each step. Raman scattering on a $1s^2S$ state can therefore lead to either ns^2S or nd^2D states. To find a total scattering cross-section in terms of commonly used oscillator strengths, we sum the differential cross-sections (5) over all angular momentum eigenstates and the polarisation directions, and integrate over all angles between incident and scattered photon. In addition, we express dipole matrix elements as functions of the corresponding weighted oscillator strengths. The resulting scattering cross-section is

$$\sigma_{(1s\to nl)}^{(\mathrm{Raman})} = A\cdot\sigma_e\,\nu_i\nu_f^3\left|\sum_m \sqrt{\frac{(gf)_{fm}}{\nu_{fm}}}\sqrt{\frac{(gf)_{1m}}{\nu_{1m}}}\,\frac{(\nu_{1m}+\nu_{fm})}{(\nu_{1m}-\nu_i)\,(\nu_{fm}+\nu_i)}\right|^2. \quad (7)$$

σ_e is defined as the Thomson cross-section, and its value is $\sigma_e = \dfrac{8\pi e^4}{3m_e^2c^4} = 6.65\ 10^{-25}\,\mathrm{cm}^2$. For $1s\to ns$ and $1s\to nd$ transitions the coefficient A is given by

$$A = \frac{1}{16}. \quad (8)$$

The weighted oscillator strength is defined as

$$(gf)_{ik} = g_i f_{ik} = -g_k f_{ki}\,. \quad (9)$$

Rayleigh scattering is the special case, where final and initial states of the atom are identical, thus emitted and absorbed photons have the same energy: $h\nu_i = h\nu_f$. In this case the scattering cross-section reduces to

$$\sigma_R(\lambda) = \sigma_e\left[\sum_k \frac{f_{1k}}{\left(\frac{\lambda}{\lambda_{1k}}\right)^2-1}\right]^2. \quad (10)$$

The sum in expression (10) includes the oscillator strengths f_{1k} of the hydrogen Lyman lines, where λ_{1k} are the corresponding wavelengths. In formulae (7) and (10) we do not include the effects of continuum states. In our case this is justified, as we are only interested in $1215\,\text{Å} < \lambda < 2000\,\text{Å}$, where continuum contributions can still be neglected. An estimate of the error may be obtained from Fig. 2 of Nussbaumer et al. (1989). Note that expression (10) agrees with formula (49,15) of Unsöld (1968). However, his formula (49,16) should be quadratic in Σf_r, similarly the formula given by Mihalas (1978) deviates from expression (10).

Our numerical calculations, mentioned at the beginning of Sect. 3.1 have shown that Thomson-scattering by free electrons, as well as absorption by hydrogen are of minor importance as opacity sources at the wavelengths considered; they can therefore be neglected. As long as Si is ionized, the photoionization of metals can also be neglected. If H^- is present, it can absorb very strongly. However, in the inner part of the wind the relatively high radiation temperature prevents formation of H^- with its ionization potential of 0.75 eV, and in the outer part of the wind the production rate is limited by the number of available electrons.

3.2. An analytical solution

In Sect. 2 we defined s as the radial distance of a line of sight from the center of the star. We now express the impact parameter in units of stellar radii

$$b = \frac{s}{R_*}. \quad (11)$$

As before, t stands for the distance along the line of sight, thus $t = \sqrt{r^2-s^2}$. We also define an effective eclipse radius b_λ in the sense that for a given wavelength λ

$$\tau_\lambda(b_\lambda) = 1\,. \quad (12)$$

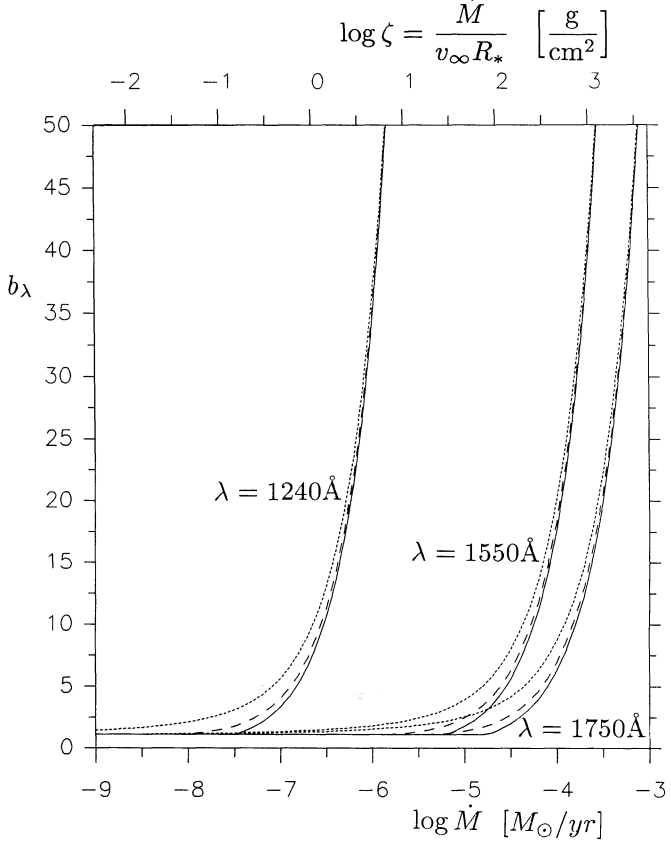

Fig. 1. Effective relative radii b_λ. They are shown as a function of $\dot{M}$ for $v_\infty = 20\,\mathrm{km\,s^{-1}}$ and $R_* = 100\,R_\odot$ for the three wavelengths 1240 Å, 1550 Å, and 1750 Å. The solid line represents $\beta = 0$, the broken line $\beta = 1$, and the dotted line $\beta = 4$. For $\beta = 0$ the radius b_λ is also given as a function of the scaling parameter ζ

Thus in practice b_λ is the relative size – in terms of eclipsing effect – of the star at wavelength λ. We have studied the eclipse effects for a grid of mass-losses and stellar radii. The numerical calculations show that:

(a) When model atmospheres of Scholz are employed the difference in b_λ between Miras and ordinary red giants are small for all λ.

(b) b_λ has very similar values when the model atmosphere of Scholz is replaced by an optically thick sphere of radius R_*, we therefore set $\tilde{R} = R_*$.

These results, together with the fact that Rayleigh scattering is the dominant shielding mechanism, allow an analytical representation of b_λ. We now derive that formula. The optical depth in the continuum, due to Rayleigh scattering is:

$$\tau(b) = \int_{-\infty}^{\infty} \frac{\sigma_R \dot{M}}{4\pi\,\mu m_\mathrm{H}\, v(r)\, r^2}\, dt\,. \tag{13}$$

For an outflow velocity of the form

$$v(r) = v_\infty \left(1 - \frac{R_*}{r}\right)^\beta, \tag{14}$$

the optical depth can be calculated analytically if β is an integer. For the case of $\beta = 1$ we obtain

$$\tau(b) = \frac{\sigma_R}{2\pi\,\mu m_\mathrm{H}} \frac{\dot{M}}{v_\infty R_*} \frac{1}{\sqrt{b^2-1}} \left[\arcsin\frac{1}{b} + \frac{\pi}{2}\right]. \tag{15}$$

For a constant outflow velocity

$$v(r) = v_\infty\,, \tag{16}$$

which corresponds to $\beta = 0$, the relative radius for which the optical depth along the line of sight reaches $\tau_\lambda = 1$ is

$$b_\lambda = \max\left[\frac{\sigma_R}{4\mu m_\mathrm{H}} \frac{\dot{M}}{v_\infty R_*},\, 1\right]. \tag{17}$$

In Fig. 1 we show b_λ for $\beta = 0$, 1 and 4 for a particular choice of R_* and v_∞, and also as a function of the scaling parameter

$$\zeta = \frac{\dot{M}}{v_\infty R_*}. \tag{18}$$

Due to the behaviour of $\sigma_R(\lambda)$ the effective radius strongly increases with decreasing λ. Because of its influence on the density structure the β-dependence can lead to differences of about a factor 2 in b_λ between $\beta = 0$ and $\beta = 4$. As can also be seen from expression (17) the effective radius increases linearly with $\dot{M}$. Thus, once an optical depth of 1 is reached, a further growth in mass-loss leads to a rapid increase in the effective radius of the star. Typical mass-losses for red giants in symbiotic stars reach from 10^{-7} up to $10^{-4}\,M_\odot\,\mathrm{yr}^{-1}$ (Kenyon et al., 1988).

The velocity structure in the winds of cool giants is not known. In a dust driven wind the velocity is likely to remain low up to the dust formation point which lies far from the stellar surface. For our model calculations we need a velocity law which is able to describe this behaviour but also allows for constant outflow velocities. Expression (14) includes both possibilities. A dust driven wind is best approximated by a high value of β; we take $\beta = 4$.

4. Resonance absorption of C IV λ1548 by Fe^+

4.1. *Optical depth in* Fe II *λ1548.2*

In symbiotic stars the ionization structure is most probably such, that in the predominantly neutral H^0 region iron is singly ionized, whereas it will be at least doubly ionized in the H^+ region. We shall assume that sufficient radiation is present to keep all elements Z_i^* with an ionization potential lower or equal to Fe^0 singly ionized in the whole H^0 region. Due to its low dissociation energy of 0.75 eV, that same radiation field will also suppress H^-; this was already assumed in the earlier sections. For the total abundance by number of the ionized elements, relative to hydrogen, we take

$$a(Z^*) = \sum_i a(Z_i^*) = 5\ 10^{-4}. \tag{19}$$

The total number of electrons freed by ionization of the metals is therefore

$$N_\mathrm{e} = a(Z^*) \cdot N_\mathrm{H}. \tag{20}$$

We assume the total population of Fe^+ to be concentrated in the two energetically lowest terms, a^6D and a^4F. At high electron densities, $N_\mathrm{e} \gtrsim 10^6\,\mathrm{cm}^{-3}$, the levels of a^4F are populated according to a Boltzmann distribution. For lower densities the crucial level, $a^4F_{9/2}$, is populated by direct collisional excitation from the ground term, as well as collisional excitation from the ground term to all levels of a^4F, followed by radiative decay to $^4F_{9/2}$. This concentration of the a^4F population in the $J = 9/2$ level is due to the fact that radiative transition probabilities within a^4F are much higher than probabilities out of a^4F (Nussbaumer and

Storey, 1988). For the population of $a^4F_{9/2}$ in Fe^+ we thus obtain the expression (in cgs units)

$$N(^4F_{9/2}) = N(a^6D)\frac{g(^4F_{9/2})}{g(a^6D)}\, e^{-\Delta E/kT_e}\frac{1}{1+\frac{A_{tot}\cdot g(a^4F_{9/2})\sqrt{T_e}}{8.629\ 10^{-6}\Omega\cdot N_e}}. \quad (21)$$

A_{tot} is the sum of the radiative downward transition probabilities from $^4F_{9/2}$, g is the statistical weight of the corresponding term or level, Ω stands for the total collision strength between a^6D and a^4F, and ΔE for the corresponding energy difference. The atomic data are taken from Nussbaumer and Storey (1980, 1988). We can now calculate the optical depth due to the transition $\lambda 1548.2$ of Fe^+ $a^4F_{9/2} - y^4H^0_{11/2}$.

4.2. *Absorption of* C IV $\lambda 1548$

The C IV doublet at $\lambda\lambda 1548, 1551$ is emitted from the levels of the first excited term, $2p^2P^0_{1/2,3/2}$, to the ground level $2s^2S_{1/2}$. Under optically thin conditions the fluxes are expected to show a ratio of 2:1. Already the early IUE observations (e.g. Flower et al., 1979) showed discrepancies against the expected ratio. Several explanations have been forwarded: self absorption, scattering by dust, absorption of $\lambda 1548$ by the blue-shifted $\lambda 1551$ in the wind of the star (Michalitsianos et al., 1988), and resonant absorption in the Fe II transition $a^4F_{9/2} - y^4H^0_{11/2}$ at 1548.2 Å (e.g. Johansson, 1983). Here we estimate the influence of the latter process. Neglecting stimulated emission, the optical depth due to absorption in the Fe II transition $a^4F_{9/2} - y^4H^0_{11/2}$ at $\lambda_0 = 1548.2$ Å is

$$\tau_{\lambda_0}(s) = \int_{-\infty}^{\infty}\frac{1}{8\pi}\frac{g(^4H^0_{11/2})}{g(^4F_{9/2})}N(^4F_{9/2})\lambda_0^2 A_{\lambda_0}\varphi_{\lambda_t}\,dt, \quad (22)$$

where A_{λ_0} is the radiative transition probability, and φ_{λ_t} is the Doppler profile

$$\varphi_{\lambda_t} = e^{-\left(\frac{\lambda_t-\lambda_0}{\Delta\lambda_D}\right)^2}\cdot\frac{1}{\sqrt{\pi}\,\Delta\lambda_D}, \quad (23)$$

with the half width given by

$$\Delta\lambda_D = \frac{\lambda_0}{c}\sqrt{\frac{2kT_e}{M_{Fe}}}, \quad (24)$$

and

$$\lambda_t = \lambda_0\left(1-\frac{v_t}{c}\right). \quad (25)$$

v_t is the component of the expansion velocity at the position t in direction of the observer, and M_{Fe} is the mass of the iron ion. Numerical calculations show that the same simplifications of the model are possible as for the continuum. Temperature and hydrogen density in the wind are therefore assumed to obey relations (3) and (4); as before, we therefore set $\tilde{R} = R_*$. In Fig. 2 we show the function b_λ for the line center $\lambda_0 = 1548.204$ Å and for the neighbouring continuum. For the center of the line, including continuum contributions, and $\beta = 0$ the following expression is a reasonable approximation for the effective eclipse radius, defined again in the sense that $\tau_{\lambda 1548,2}(b_{\lambda 1548,2}) = 1$:

$$b_\lambda \approx \max\cdot\left[\frac{1}{2}\left(\sigma_R N(R_*)\pi R_* + \sqrt{(\sigma_R N(R_*)\,\pi R_*)^2 + K\frac{T_e^2(R_*)}{R_*}\frac{\dot{M}}{v_\infty^2}}\right), 1\right]. \quad (26)$$

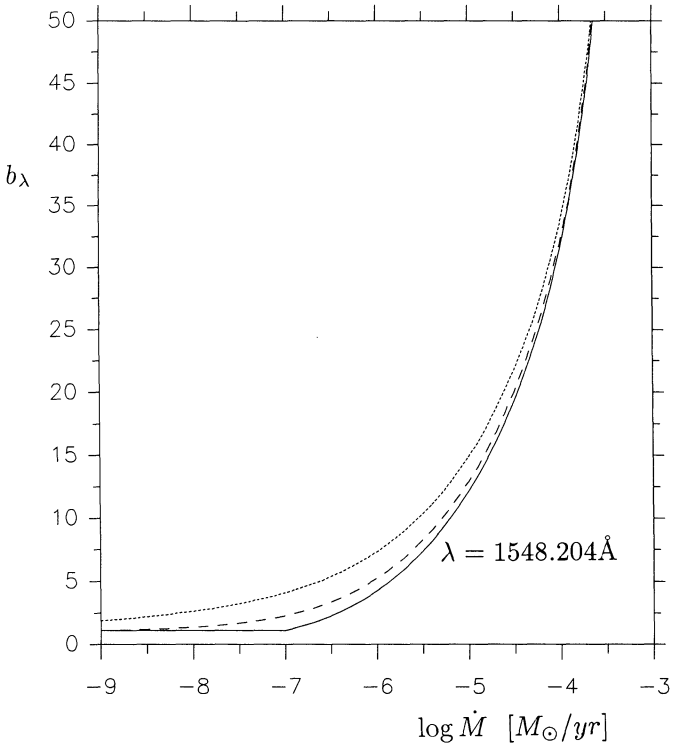

Fig. 2. The effective relative radii b_λ for the line center of Fe II $\lambda 1548.2$ are given as a function of $\dot{M}$ for $v_\infty = 20$ km s^{-1}, $R_* = 100\,R_\odot$ and $T_e(R_*) = 3000$ K. The solid line represents $\beta = 0$, the broken line $\beta = 1$, and the dotted line $\beta = 4$

The numerical factor is given by $K = 3.1$, and $\dot{M}$, R_* and v_∞ in cgs units. Because of the underlying assumptions the uncertainty in the eclipse effects in $\lambda 1548.2$ is larger than for the continuum case. The main uncertainty lies in the temperature structure $T_e(r)$ which determine $N(^4F_{9/2})$. From relation (21) we see that low values of T_e reduce the population exponentially. The uncertainty in T_e and N_e for large distances should be of minor importance. The electron density has practically no influence on $b_{\lambda 1548.2}$ because it affects $N(^4F_{9/2})$ only at low N_e which are only reached at large distances from the star in regions which contribute little to the optical depth. Uncertainties in assumptions (19) and (20) have therefore little influence on the result.

The formation of H^- greatly reduces the number of free electrons and thus of the population of the collisionally excited level $a^4F_{9/2}$. However, this occurs at distances where the particle density is sufficiently reduced to be of no concern to the calculation of τ. The inclusion of turbulence in expression (24) would have practically no influence on b_λ, as opposing effects cancel each other: Whilst turbulence is reducing local opacity, it also broadens the absorption profile. Because of the velocity structure in the cool stellar wind, this keeps the profile available for a larger number of absorbers.

5. Conclusions

Red giants and supergiants have extended atmospheres and we expect in many of them the presence of strong stellar winds. Variations in the mass-loss $\dot{M}$ will change the effective radius of the star, by which we mean the distance from the center of the star at which the optical depth of a background source is unity. In cases

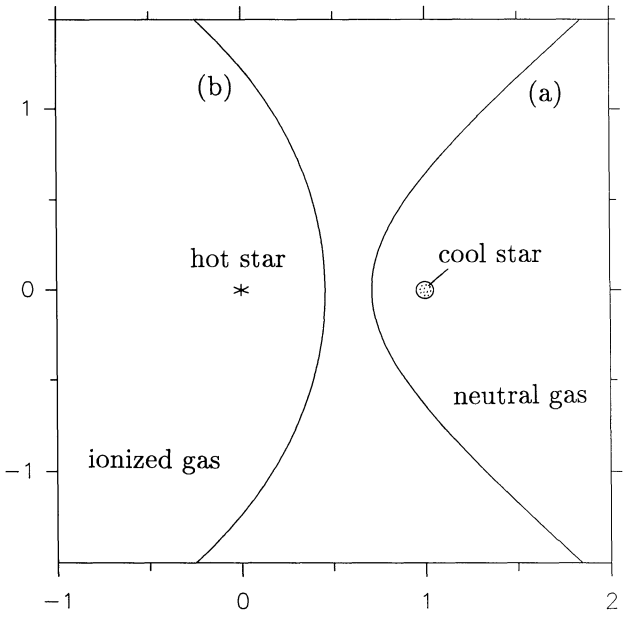

Fig. 3. Model of a symbiotic system. It consists of a cool mass-losing star and a hot star ionizing a fraction of the cool wind. With the methods described in Nussbaumer and Vogel (1987) two ionization boundaries (a) and (b) have been calculated, they separate the H^+ from the H^0 region. Rayleigh scattering in the neutral part of the wind can eclipse the line emitting regions in the ionized part of the wind

where opacity is governed by Rayleigh scattering, the effective stellar radius is strongly wavelength dependent. If simple formulae for mass-loss and wind velocity are assumed, it is possible to express the effective radius by an analytical formula; this has been derived in Sect. 3.1.

With an example we want to point out that observed eclipse effects might easily lead to erroneous interpretation if Rayleigh scattering is neglected. Let us assume that in a double star system a hot star with a small high excitation nebula emitting N v λ1240, N IV λ1486, and N III λ1750 is circling a cool star with an extended stellar wind, the opacity of which is governed by Rayleigh scattering. The nebular emission as well as the hot stellar continuum could well be considerably attenuated over at least half of the revolution period. From Fig. 1 we see that because of the respective wavelengths the periodic amplitude in the N v flux would be much larger than in N IV or N III. If Rayleigh scattering is neglected, the variation in the N III/N IV/N v flux ratio might be interpreted as being due to a periodic change of ionization.

Shortwards of Lyα Rayleigh scattering continues to be very effective; the opening of that wavelength region to observations will provide new means for studying the geometry of double star systems.

Symbiotic stars are obvious targets for studying effects described in this paper. BF Cygni is a prime candidate. Observations by Gonzales-Riestra et al. (1988) show the expected eclipse effects. An in-depth interpretation of those observations requires a detailed ionization model for a nebula in a double star system, this is outside the scope of the present paper. None the less we briefly comment on the main characteristics of an eclipse event. Figure 3 shows the geometrical configuration of double star system containing a mass-losing cool star, an ionizing hot star, and a partially ionized nebula. The location of the boundary line between the neutral and ionized nebular zone relative to the two stars depends mainly on $\dot{M}$ of the cool star, T^* of the hot star, and stellar separation. In symbiotic systems we expect orbits of low eccentricity. The duration of the eclipse will therefore mainly be determined by the boundary line. If it is located close to the cool star, curve (a), the eclipse can be relatively short. If it is located close to the hot star, curve (b), the eclipse may last a large fraction of the binary period. The viewing angle relative to the orbital plane will influence both duration and depth of the eclipse. At right angles no periodicity would be seen, but a fraction of the nebular emission could be permanently shielded from us. In BF Cygni the eclipse lasts longer than half of the binary period. This indicates heavy mass-loss, resulting in a configuration similar to curve (b). From Gonzales-Riestra et al. (1988) minimum to maximum flux ratios for some lines can be read. The wavelength dependence of most emission lines in the IUE SWP wavelength range can be well explained with the theoretically expected behaviour described in this paper. A rather high mass-loss of $\dot{M} \approx 10^{-5} M_\odot \,\mathrm{yr}^{-1}$ is required. Qualitatively this result agrees with the high mass-loss implied by the long duration of the eclipse.

Although changes in the flux ratio of the C IV doublet observed in many nebulae will probably often be due to self absorption, there may be cases where resonance absorption by Fe^+ is active. This effect can be estimated from Fig. 2.

It must be stressed that our estimates of effective radii only include the effect of Rayleigh scattering. Because of its rapid decrease with increasing wavelengths this process is only of importance for $\lambda \lesssim 2000$ Å. For longer wavelengths molecular band absorption may become dominant. Below 2000 Å the effect of H^- might have to be considered as well. In the absence of an external radiation field conditions in extended stellar atmospheres and winds of cool stars are favourable for the formation of H^-. Opacity could then well be dominated by bound-free absorption of H^- or photoionization by neutral atoms such as Si.

References

Flower, D.R., Nussbaumer, H., Schild, H.: 1979, *Astron. Astrophys.* **72**, L1

Gonzales-Riestra, R., Cassatella, A., Fernandez-Castro, T.: 1988, ESA SP-281, Vol. 1, p. 373

Johansson, S.: 1983, *Monthly Notices Roy. Astron. Soc.* **205**, 718

Kenyon, S.J., Fernandez-Castro, T., Stencel, R.E.: 1988, *Astron. J.* **95**, 1817

Michalitsianos, A.G., Kafatos, M., Fahey, R.P., Viotti, R., Cassatella, A., Altamore, A.: 1988, *Astrophys. J.* **331**, 477

Mihalas, D.: 1978, *Stellar Atmospheres*, 2nd ed., Freeman, San Francisco

Nussbaumer, H., Schmid, H.M., Vogel, M.: 1989, *Astron. Astrophys.* **211**, L27

Nussbaumer, H., Storey, P.J.: 1980, *Astron. Astrophys.* **89**, 308

Nussbaumer, H., Storey, P.J.: 1988, *Astron. Astrophys.* **193**, 327

Nussbaumer, H., Vogel, M.: 1987, *Astron. Astrophys.* **182**, 51

Scholz, M.: 1985, *Astron. Astrophys.* **145**, 251

Scholz, M., Tsuji, T.: 1984, *Astron. Astrophys.* **130**, 11

Unsöld, A.: 1968, *Physik der Sternatmosphären*, berichtigte 2. Aufl., Springer, Berlin, Heidelberg, New York